NUMERICAL MODELLING OF CRACK GROWTH IN DUCTILE DAMAGING MATERIALS

M. FEUCHT*, H. BAASER*, J. HOHE*, D. GROSS*

Ductile crack growth under quasi-static conditions is examined numerically using a constitutive model accounting for damage effects. The continuum model is applied by two different methods. In the first concept, the elastic-plastic crack growth problem is solved by limiting the damage zone to a narrow strip ahead of the crack tip and introduction of a Dugdale-Barenblatt-type cohesive zone model. In the second concept the damage model is implemented directly into a two dimensional elastic-plastic finite element for the plain strain case. Both concepts are applied to examine the ductile crack growth in a CT-specimen. A good agreement of the numerical results with experimental data available in literature is observed.

INTRODUCTION

The specimen size and geometry dependence of the crack resistance curves is a well known problem in the analysis of ductile crack growth. To deal with this problems several concepts have been developed in literature. Macromechanical approaches introduce additional fracture parameters while micromechanical concepts attempt to incorporate the failure process into the constitutive description of the material. Therefore no external fracture criterion is required in this kind of approach.

One of the most successful damage models is the model originally presented by Gurson (2) which describes the ductile failure process by nucleation, growth and coalescence of microvoids. In the present study this model is employed in modified form as given by Tvergaard and Needleman (7).

* Institut für Mechanik, Technische Hochschule Darmstadt.

GURSON'S DAMAGE MODEL

Gurson's model in modified form as given by Ref. (7) uses the yield condition

$$\Phi = \frac{\sigma_e^2}{\sigma_M^2} + 2q_1 f^* \cosh\left(\frac{\sigma_{kk}}{2\sigma_M}\right) - \left(1 + (q_1 f^*)^2\right) = 0 \tag{1}$$

where

$$f^* = \begin{cases} f & \text{if: } f \leq f_c \\ f_c + \dfrac{1/q_1 - f_c}{f_f - f_c}\,(f - f_c) & \text{if: } f > f_c \end{cases} . \tag{2}$$

Here, σ_{ij} denotes the macroscopic stress tensor, σ_e the macroscopic equivalent stress, σ_M the actual yield stress of the matrix material, f the real and f^* the effective void volume fraction respectively; q_1, f_c and f_f are material parameters. The void volume rate is assumed to consist on the growth of existing microvoids and the nucleation of new voids:

$$\dot{f} = (1 - f)\,\dot{\varepsilon}_{kk}^{pl} + \mathcal{A}\,\dot{\varepsilon}_M^{pl} \tag{3}$$

where a dot denotes the partial differentiation with respect to time. The first term in eq. (3) can be derived from the condition of plastic incompressibility of the matrix material, while the usual statistical approach is used for the nucleation term (see Tvergaard (6)):

$$\mathcal{A} = \frac{f_N}{s_N\sqrt{2\pi}}\, e^{-\frac{1}{2}\left(\frac{\varepsilon_M^{pl} - \varepsilon_N}{s_N}\right)^2} \dot{\varepsilon}_M^{pl}. \tag{4}$$

Here $\dot{\varepsilon}_M^{pl}$ denotes the equivalent plastic strain rate of the matrix material and f_N, ε_N, s_N are material parameters describing the nucleation of microvoids. The total plastic strain rate is splitted additive into an elastic part governed by Hooke's law and a plastic part for which an associated flow rule is assumed. An evolution equation for the equivalent plastic strain rate of the matrix material is obtained by taking into account that the macroscopic and microscopic plastic work rate must be equal:

$$\dot{\varepsilon}_M^{pl} = \frac{\sigma_{ij}\dot{\varepsilon}_{ij}^{pl}}{(1 - f)\sigma_M} \tag{5}$$

Finally, a Power-law hardening matrix material is adopted.

NUMERICAL CONCEPTS

Cohesive Zone Formulation

According to Zhang and Gross (8),(9) the constitutive equations (1) - (5) can be rewritten after some manipulations by introduction of a macroscopic equivalent plastic strain rate $\dot{\varepsilon}_e^{pl}$ defined in the usual way (see e.g. Ref. (8)). Using

$\dot{\varepsilon}_e^{pl}$ and the condition that the macroscopic plastic work rate must be equal to the microscopic plastic work rate, a system of ordinary differential equations is obtained, which can be simplified under the assumption of equivalence of micro- and macroscopic strain to the following cohesive stress-strain relationship (see Ref. (9) for details):

$$\sigma_{coh} = c_\sigma(1 - q_1 f^*)\,\sigma_0 \left(\frac{c_\sigma \varepsilon_{coh}}{\varepsilon_0}\right)^{\frac{1}{N}} \tag{6}$$

$$\frac{\partial f}{\partial \varepsilon_{coh}} = c_\sigma \left(\frac{3}{2} q_1 f^* \frac{1-f}{1-q_1 f^*} \sinh\left(\frac{c_f}{2}(1 - q_1 f^*)\right) + \mathcal{D}\right) \tag{7}$$

where

$$c_\sigma = \begin{cases} 1 & \text{for plain stress} \\ \frac{2}{3}\sqrt{3} & \text{for plain strain} \end{cases}, \quad c_f = \begin{cases} 1 & \text{for plain stress} \\ \sqrt{3} & \text{for plain strain} \end{cases}$$

The obtained constitutive equations (6),(7) are now implemented in one-dimensional finite spar elements which are used to define the cohesive zone in a finite element discretization. The area outside of the cohesive zone is discretized by elastic-plastic triangular displacement elements with biquadratic shape functions. The material in this area is assumed to be governed by standard non-damaging v. Mises J_2-plasticity with power-law hardening material.

Direct Finite Element Implementation

In contrast to the cohesive zone model where a simplified one-dimensional version of the Gurson model is used, the damage model is now implemented directly into plane strain finite elements. Here, the key point for the implementation of the constitutive equations (1) - (5) is the choice of the integration scheme. Efficient schemes are needed, which are fast and accurate. There are, in general, explicit schemes (cf. Ortiz (4)), which have the advantage of easy derivation and implementation. On the other hand they are instable and very small time steps are necessary to obtain an accurate solution. Consequently, implicit algorithms became very important in the last years because of their stability and good accuracy even for large time steps (cf. Aravas (1), Zhang and Niemi (10)). Simo (5) showed that the multi-step algorithms in general do not cause much improvement in the accuracy of the solution but have a minor range of stability in comparision to single-step schemes. In Ref. (10) the generalized mid-point algorithm for the gurson model is examined in particular and the Euler backward algorithm is found to be the best choice.
For these reasons the implicit Euler backward scheme has been chosen in the present study, in which the problem to be adressed is that of updating the known state variables $\varepsilon_{ij}, \varepsilon_{ij}^{pl}, \sigma_{ij}, f$ and ε_M^{pl} on the actual time increment. For

this purpose it is useful to introduce two scalar variables

$$p = -\frac{1}{3}\sigma_{kk} \qquad q = \sqrt{\frac{3}{2}s_{ij}s_{ij}}, \tag{8}$$

where s_{ij} denotes the stress deviator. The Lagrange multiplicator rate $\dot{\gamma}$ is splitted into a pressure dependent and a part independent of the hydrostatic stress

$$\Delta\varepsilon_p = -\dot{\gamma}\frac{\partial\Phi}{\partial p} \qquad \Delta\varepsilon_q = \dot{\gamma}\frac{\partial\Phi}{\partial q} \tag{9}$$

so that all variables of the equation system (1) - (5) can be expressed in terms of four unknown increments $\Delta\varepsilon_p, \Delta\varepsilon_q, \Delta f, \Delta\varepsilon_M^{pl}$. The following nonlinear system of equations, which has to be solved on each Gaussian point, is obtained:

$$0 = \Phi \tag{10}$$

$$0 = \Delta\varepsilon_p\frac{\partial\Phi}{\partial q} + \Delta\varepsilon_q\frac{\partial\Phi}{\partial p} \tag{11}$$

$$0 = \Delta f - (1-f)\Delta\varepsilon_p - A\varepsilon_M^{pl} \tag{12}$$

$$0 = \Delta\varepsilon_M^{pl} - \frac{-p\Delta\varepsilon_p + q\Delta\varepsilon_q}{(1-f)\sigma_M} \tag{13}$$

The system of equations is solved by Newton's method, where the consistent tangent moduli are derived following the suggestions in Ref. (1) and (10). During the constitutive calculations, where stress and state variables are updated, the total strain is known. The elasticity equation yields

$$\sigma_{ij}^{t+\Delta t} = C_{ijkl}(\varepsilon_{kl}^{t+\Delta t} - \varepsilon_{kl}^{t,p}) - K\Delta\varepsilon_p\delta_{ij} - 2G\Delta\varepsilon_q n_{ij} \tag{14}$$

where $n_{ij} = 3s_{ij}/2q$ and K, G being the elastic bulk and shear modulus, respectively. The derivation of the consistent elastoplastic tangent moduli requires the exact linearization of eq. (14) as:

$$d\sigma_{ij} = C_{ijkl}d\varepsilon_{kl} - Kd(\Delta\varepsilon_p)\delta_{ij} - 2Gd(\Delta\varepsilon_q)n_{ij} - 2G\Delta\varepsilon_q\frac{\partial n_{ij}}{\partial\varepsilon_{kl}}d\varepsilon_{kl} \tag{15}$$

where $\partial n_{ij}/\partial\varepsilon_{kl}$ is given by

$$\frac{\partial n_{ij}}{\partial\varepsilon_{kl}} = \frac{G}{q^{tr}}(3\delta_{ik}\delta_{jl} - \delta_{ij}\delta_{kl} - 2n_{ij}n_{kl}) \tag{16}$$

and $d(\Delta\varepsilon_p), d(\Delta\varepsilon_q)$ can be determined by the solution of a linear system of equations as given by Ref. (1) or (10). Finally the following explicit expression for the consistent tangent moduli is obtained:

$$\frac{\partial\sigma_{ij}}{\partial\varepsilon_{kl}} = d_1\,\delta_{ij}\delta_{kl} + d_2\,\delta_{ik}\delta_{jl} + d_3\,n_{ij}n_{kl} + d_4\,\delta_{ij}n_{kl} + d_5\,n_{ij}\delta_{kl} \tag{17}$$

with the scalar values $d_1 - d_5$ as defined in Ref. (10).

RESULTS

The methods presented in the previous section are applied to examine ductile crack growth in a CT-specimen (see Fig. (2)). The upper half of the specimen is discretized as presented in Fig. (1). The material parameters are chosen as suggested in Ref. (3). Exemplary the displacement v_{ll} of the crack surfaces on the load line is plotted as function of the crack propagation Δa in Fig. (3). Experimental results (Ref. (3)) have been added for comparison.
A good agreement of the results obtained by the different numerical models presented in this paper can be observed as well as a qualitative agreement to experimental data. The agreement of the curves resulting from the two numerical approaches can be explained by the fact that significant damage of the material occurs only in the narrow zone ahead of the crack tip. Therefore it is demonstrated that the rather simple cohesive zone model used in the present study is able to simulate the physical effects of crack propagation in a CT-specimen. Nevertheless, for problems in which the crack propagation path is not known a priori, a more general formulation of the damage model is required as presented in the second approach of this study. The remarkable advantage of the cohesive model concerning the needed computing time has to be emphasized.

REFERENCES

(1) Aravas, N., Int. J. Num. Meth. Eng., Vol. 24, 1987, pp.1395-1416.

(2) Gurson, A.L., J. Eng. Mat. Tech., Vol. 99, 1977, pp. 2-15.

(3) Klingbeil, D.,Künecke G. and Schicker, J.,"On the Application of Gurson's Model to Various Fracture Mechanics Specimens", Report BAM-1.31 93/3, Laboratory 1.31, BAM Berlin, 1993.

(4) Ortiz, M. and Simo, J.C., Int. J. Num. Eng., Vol. 23, 1986, pp.353-366.

(5) Simo, J.C., "Topics on the Numerical Analysis and Simulation of Plasticity", E. Science Publishers B.V., North Holland, to appear.

(6) Tvergaard, V., Advances in Appl. Mech., Vol. 27, 1989,pp. 83-151

(7) Needleman, A. and Tvergaard V., Eng. Frac. Mech., Vol. 47, 1994, pp. 75-91.

(8) Zhang, Ch. and Gross, D., "Analysis of Ductile Crack Growth by a Simple Damage Model", Transactions of the 12th International Conference on Structural Mechanics in Reactor Technology. Edited by K. Kussmaul, Elsevier Science Publishers, Amsterdam, 1993.

(9) Zhang, Ch. and Gross, D., Eng. Frac. Mech., Vol. 47, 1994, pp. 237-248.

(10) Zhang, Z.L and Niemi, E., Int. J. Num. Meth. Eng., Vol. 38, 1995, pp. 2033-2053.

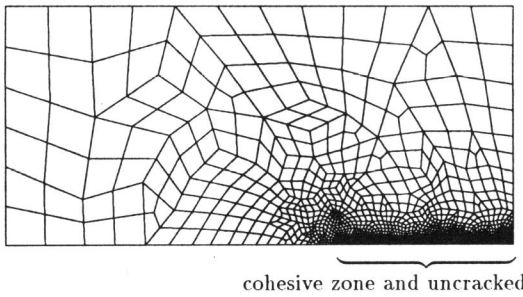

Figure 1: Discretization of CT-Specimen

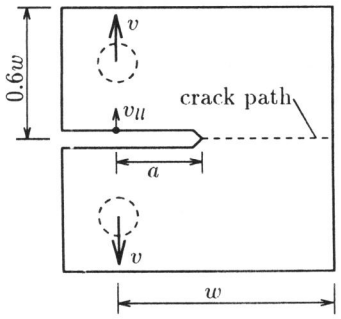

Figure 2: Geometry of CT-Specimen (w=50mm, a=29.5mm)

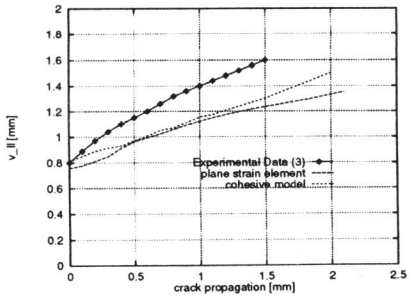

Figure 3: Displacement v_{ll} vs crack propagation Δa